

Supplementary Information

Nitrogen-doped carbon nanoparticles derived from acrylonitrile plasma for electrochemical oxygen reduction

Gasidit Panomsuwan,^{*a} Nagahiro Saito^{bcd} and Takahiro Ishizaki^{ad}

^a *Department of Materials Science and Engineering, Faculty of Engineering, Shibaura Institute of Technology, Tokyo 135-8548, Japan*

^b *Department of Materials, Physics and Energy Engineering, Graduate School of Engineering, Nagoya University, Nagoya 464-8603, Japan*

^c *Green Mobility Collaborative Research Center, Nagoya University, Nagoya 464-8603, Japan*

^d *Core Research for Evolutional Science and Technology (CREST), Japan Science and Technology Agency (JST), Saitama 333-001, Japan.*

*Corresponding author

Gasidit Panomsuwan

Department of Materials Science and Engineering, Faculty of Engineering, Shibaura Institute of Technology, 3-7-5 Toyosu, Koto-ku, Tokyo 135-8548, Japan

Tel: +81-3-5859-8115

Fax: +81-3-5859-8101

E-mail: i036050@sic.shibaura-it.ac.jp; g.panomsuwan@gmail.com

Experimental section

Chemicals

Acrylonitrile (C_3H_3N , purity 99.5%), ethanol (C_2H_5OH , purity 99.5%), methanol (CH_3OH , purity 99.8%), and 0.1 M potassium hydroxide (KOH) aqueous solution were purchased from Kanto Chemical Co., Inc. Nafion® DE 521 solution (5 wt% in mixture of lower aliphatic alcohols and water, contains 45% water) and 20 wt% Pt on Vulcan XC-72 (20% Pt/C) were purchased from Sigma-Aldrich. Potassium hexacyanoferrate (III) ($K_3[Fe(CN)_6]$, purity 99.0%) was purchased from Wako Pure Chemical Industries. All of the reagents were of analytical grade and used without further purification. Ultrapure water (18.2 M Ω -cm at 25 °C) was obtained by purification with an Advantec RFD250NB system.

Synthesis of nitrogen-doped carbon nanoparticles

Fig. S1 shows a schematic illustration of the solution plasma system used for synthesizing the nitrogen-doped carbon nanoparticles in this study. The 1 mm diameter tungsten wire (purity 99.9%, Nilaco Corporation) was used as the electrodes, which were shielded with an insulating ceramic tube. A pair of tungsten electrodes was placed at the center of a glass reactor with a gap distance of 1.0 mm. A bipolar high-voltage pulse of ~ 1.5 kV was applied to the tungsten electrodes using a MPP-HV04 Pekuris bipolar pulse generator. The pulse duration and repetition frequency were fixed at 1 μ s and 20 kHz, respectively. Plasma was generated and maintained in 100 mL of liquid acrylonitrile under vigorous stirring for 30 min. Once the plasma was generated at the gap between the electrodes, the formation of carbon particles was readily observed. After the synthesis, the carbon particles were separated by filtration followed by several washes with ethanol to remove soluble organic compounds. Then, the as-synthesized carbon samples were dried at 60 °C for 12 h. The dried samples were uniformly ground and transferred into a quartz tube inside the furnace. The samples were annealed at different temperatures from 500 to 900 °C for 1 h with a heating rate of 5 °C min⁻¹ under Ar flow rate of 0.5 L min⁻¹ after excluding air by flowing Ar for 30 min. The samples were collected after naturally cooling to room temperature under same environment.

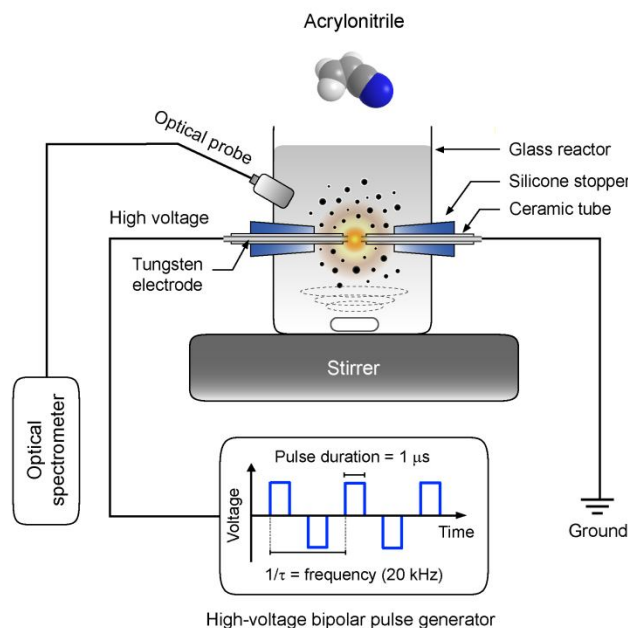


Fig. S1 Schematic illustration of experimental setup for the solution plasma synthesis of nitrogen-doped carbon nanoparticles from liquid acrylonitrile in this study.

Characterizations

Transmission electron microscopy (TEM) images, high-resolution TEM images, selected area electron diffraction (SAED) patterns, and energy dispersive spectroscopy (EDS) elemental mapping images were acquired using a JEOL JEM-2500SE at an accelerating voltage of 200 kV. Dried carbon sample was dispersed in ethanol under ultrasonication for 15 min. Then, the suspension was dropped onto a 150 mesh copper TEM grid and let the solvent evaporation for 24 h prior to the investigation. Nitrogen adsorption was collected on a Micrometrics Gemini 2375 instrument equipped with a VacPrep 061 at 77 K to investigate the specific surface area. The samples were degassed at 100 °C for 12 h under vacuum before the measurements. Specific surface area was determined using the Brunauer-Emmett-Teller (BET) method in the relative pressure (P/P_0) range of 0.05–0.30. Elemental analysis (EA) of carbon, hydrogen, and nitrogen was performed on a Perkin Elmer 2400 Series II CHNS/O elemental analyzer. The phase structure was identified using a Rigaku Ultima IV X-ray diffractometer with monochromatic Cu $K\alpha$ radiation ($\lambda = 0.15418$ nm) operating at 40 kV and 40 mA (1.6 kW). Raman spectra were recorded on a JASCO NRS-5100 Raman spectrometer equipped with a laser-excitation wavelength of 532.1 nm. X-ray photoelectron spectroscopy (XPS) measurements were carried out on a JEOL JPS-9010MC using monochromatic Mg $K\alpha$ radiation (1253.6 eV) as an excitation source. The emission current and anode voltage were operated at 25 mA and 10 kV, respectively. The binding energy was calibrated using the C 1s peak (284.5 eV). The relevant fitting

curves were analyzed using a Gaussian line shape and Shirley background subtraction. The measurement was carried out under ultra high vacuum conditions at a base pressure of 2×10^{-6} Pa.

Optical emission spectroscopy measurement

Optical emission spectrum of the plasma generated in a liquid acrylonitrile was recorded with an Avantes AvaSpec-3648 fiber optic spectrometer system in the wavelength range of 300 to 700 nm. The spectrum was recorded by averaging 3 scans with a 200 ms integration time. The optical probe was set 15 mm above the plasma zone.

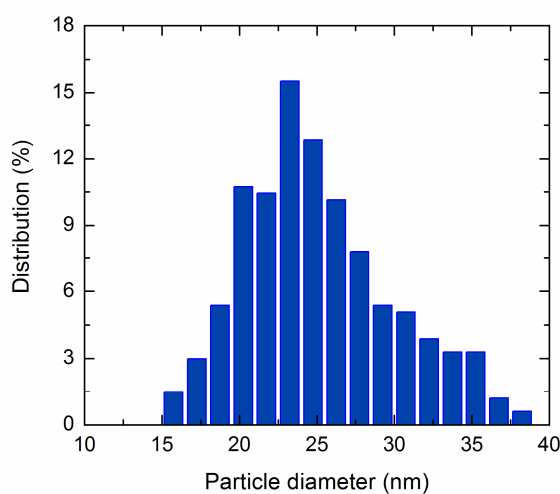


Fig. S2 Particle size distribution of NCNP-800 deduced from bright-field TEM images (300 particles).

Table S1 Summary of bulk and surface elemental compositions of the catalysts annealed at different temperatures.

Sample	Bulk elemental composition EA (wt%)			Surface elemental composition XPS (at%)		
	C	H	N	C	O	N
NCNP	82.34	1.20	3.18	85.32	9.90	4.78
NCNP-500	85.67	0.65	1.96	91.70	5.52	2.78
NCNP-600	86.47	0.40	1.51	90.60	7.16	2.24
NCNP-700	85.93	0.25	1.25	93.58	4.76	1.66
NCNP-800	86.36	0.12	1.06	94.08	4.49	1.43
NCNP-900	87.12	0.09	0.93	93.81	4.86	1.33

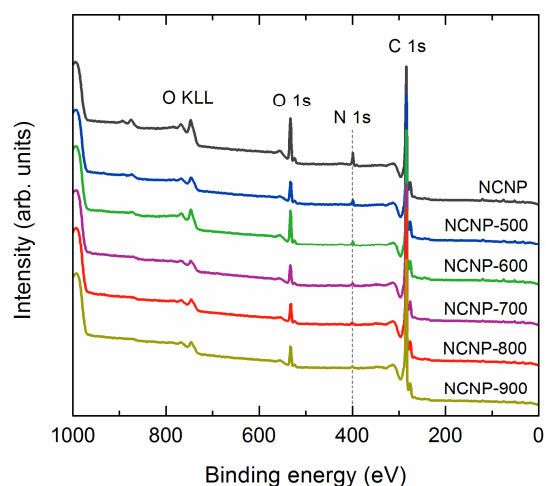


Fig. S3 XPS survey spectra of the catalysts annealed at different temperatures. The vertical dashed line indicates the position of N 1s peak.

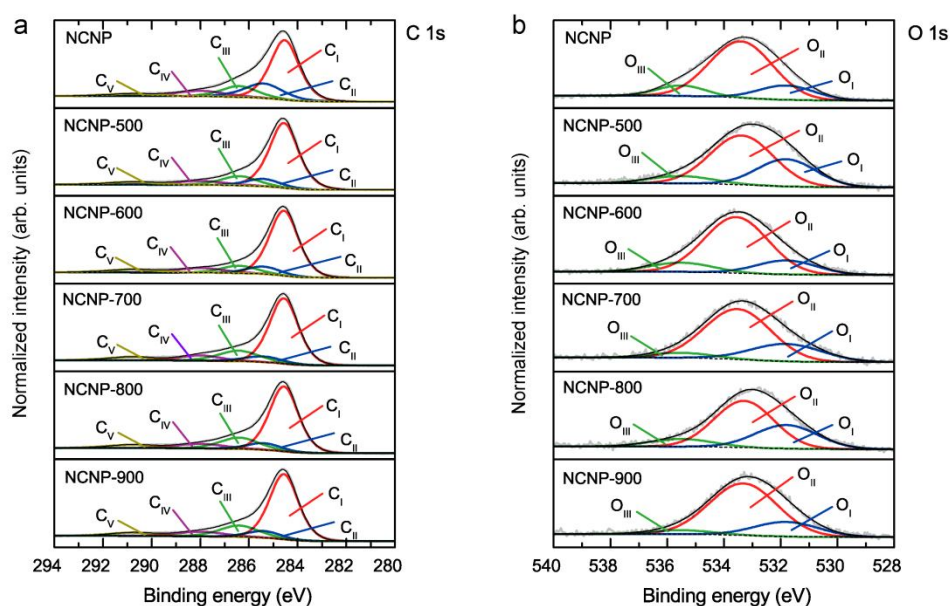


Fig. S4 High-resolution XPS spectra of (a) C 1s and (b) O 1s spectra of the catalysts annealed at different temperatures. The high-resolution XPS C 1s spectra can be divided into five peaks. The most pronounced peak at 284.5 ± 0.1 eV (C_I) is evidence that the carbons are present in the sp^2 graphite structural form. The other four peaks at the tail of asymmetric XPS C 1s peak are likely due to the presence of C sp^3 bond (C_{II} : 285.4 ± 0.2 eV), C–O/C=N (C_{III} : 286.4 ± 0.2 eV), C=O/C–N (C_{IV} : 288.0 ± 0.1 eV), and C=O bonds of different types (carbonyl, aldehyde, *etc.*) (C_V : 290.7 – 291.9 eV).^{S1–S3} The high-resolution XPS O 1s can be deconvoluted into three components from C=O/O–C=O (O_I : 531.8 ± 0.1 eV), C–O–C/COOH/C–OH (O_{II} : 533.4 ± 0.2 eV), and adsorbed molecular water (O_{III} : 535.5 ± 0.1 eV).^{S3,S4}

Table S2 Relative percentage of various bonding states of carbon and oxygen derived from the deconvolution of high-resolution XPS C 1s and O 1s spectra, respectively (Fig. S4a and S4b).

XPS peak	Catalyst						
	NCNP	NCNP-500	NCNP-600	NCNP-700	NCNP-800	NCNP-900	
C 1s	C–C sp ²	56.50%	67.56%	68.27%	64.93%	65.56%	64.23%
	sp ³	18.42%	8.94%	9.10%	7.44%	7.67%	7.77%
	C=O/C–N	12.84%	12.02%	9.64%	14.62%	14.32%	15.07%
	C–O/C=N	8.80%	7.03%	8.06%	7.44%	7.38%	7.68%
	COOH	3.44%	4.45%	4.93%	5.57%	5.07%	5.25%
O 1s	C=O	16.37%	30.86%	16.80%	25.12%	30.99%	19.79%
	C–OH	73.37%	60.37%	71.62%	68.45%	58.87%	74.87%
	C–OO	10.26%	8.77%	11.58%	6.43%	10.14%	5.34%

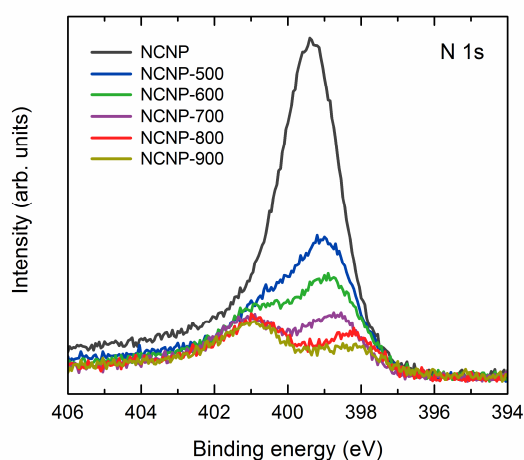


Fig. S5 Comparison of high-resolution XPS N 1s spectra of the catalysts annealed at different temperatures.

Table S3 Relative percentage and content of various nitrogen bonding states (in parentheses) of all catalysts derived from a careful deconvolution of high-resolution XPS N 1s spectra.

XPS peak	Catalyst						
	NCNP	NCNP-500	NCNP-600	NCNP-700	NCNP-800	NCNP-900	
N 1s	Pyridinic-N	8.37% (0.40 at%)	15.67% (0.44 at%)	20.04% (0.45 at%)	38.56% (0.64 at%)	35.02% (0.50 at%)	31.23% (0.41 at%)
	Nitrile-N	62.05% (2.97 at%)	48.71% (1.35 at%)	34.90% (0.78 at%)	5.61% (0.09 at%)	-	-
	Pyrolic-N	15.13% (0.72 at%)	12.38% (0.34 at%)	13.35% (0.30 at%)	11.61% (0.19 at%)	1.63% (0.02 at%)	-
	Graphitic-N	9.58% (0.46 at%)	15.44% (0.43 at%)	23.36% (0.52 at%)	34.37% (0.57 at%)	53.13% (0.76 at%)	56.30% (0.75 at%)
	Pyridinic-N oxide	4.87% (0.23 at%)	7.80% (0.22 at%)	8.35% (0.19 at%)	9.85% (0.16 at%)	10.22% (0.15 at%)	12.47% (0.17 at%)

Electrochemical measurements

Preparation of catalyst inks

The catalyst ink was prepared by dispersing 5 mg of finely ground catalyst in a mixture containing 480 μL of ultrapure water, 480 μL of ethanol, and 40 μL of Nafion® DE 521 aqueous solution followed by ultrasonication until a homogeneous dispersion was obtained.

Preparation of catalyst-modified electrodes

A glassy carbon (GC) rotating disk electrode (RDE) was polished with 0.1 μm diamond slurry followed by 0.05 μm alumina suspension on a polishing pad in order to obtain the mirror electrode surface. After that, the GC-RDE was ultrasonically cleaned in ultrapure water for 5 min to remove residual alumina, subsequently rinsed with ethanol and ultrapure water, and finally blown dried by N_2 gun. A certain amount of 5 μL of the well-dispersed catalyst ink was loaded onto a GC-RDE (ALS, Co., disk diameter: 4 mm, $A = 0.126 \text{ cm}^2$), yielding a catalyst loading of about $0.2 \text{ mg}_{\text{cat}} \text{ cm}^{-2}$. Then, the catalyst-modified electrodes were dried in air for 6 hr at room temperature prior to the electrochemical measurements. For comparison, a commercial 20% Pt/C catalyst was modified on a GC-RDE using the same procedure with a catalyst loading of about $0.2 \text{ mg}_{\text{cat}} \text{ cm}^{-2}$ ($40 \mu\text{g}_{\text{Pt}} \text{ cm}^{-2}$).

Electrochemical measurements

The electrochemical measurements were carried out on an ALS-CH model 704ES electrochemical analyzer (CH instruments Inc.) equipped with a rotating ring disk electrode apparatus (RRDE-3A, ALS Co.) in a three-electrode beaker cell. A Pt coil (ALS, Co.) and Ag/AgCl electrode filled with saturated KCl aqueous solution (ALS, Co.) were used as the counter and reference electrodes,

respectively. All electrochemical measurements were performed in a 0.1 M KOH solution at room temperature (25 ± 1 °C).

Cyclic voltammetry (CV) measurements were performed on a catalyst-modified GC-RDE in both N_2 and O_2 saturated 0.1 M KOH solutions. Prior to the measurements, 0.1 M KOH solution was purged with high purity N_2 or O_2 gases at a constant flow rate of 50 mL min^{-1} for at least 30 min to ensure saturation of N_2 or O_2 , respectively. The stable CV curves were recorded after 30 cycles in the potential range from -1.0 to 0.2 V at a scan rate of 50 mV s^{-1} in both N_2 and O_2 -saturated 0.1 M KOH solutions. Normalized currents are given in terms of geometric area (mA cm^{-2}).

Linear sweep voltammetry (LSV) measurements were performed on a catalyst-modified GC-RDE at a scan rate of 10 mV s^{-1} and a rotation speed of 1600 rpm in an O_2 -saturated 0.1 M KOH solution (from -1.0 to 0 V). The LSV curves of all catalysts were collected after the stable CV curve was obtained.

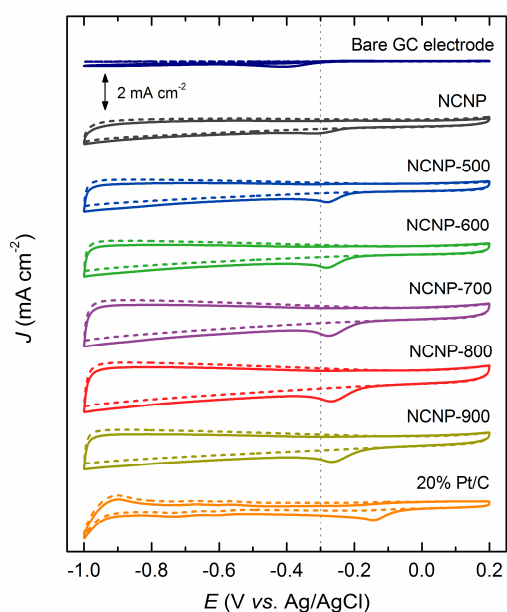


Fig. S6 CV curves of the ORR on various catalysts in 0.1 M KOH solution saturated with N_2 (dashed line) and O_2 (solid line). The dotted line is guide for the eyes indicating the ORR peak position of NCNP.

Koutecky–Levich (K–L) analysis

To study the ORR mechanisms and kinetics of the catalysts, the LSV measurements were carried out on a catalyst-modified GC-RDE in O_2 -saturated 0.1 M KOH at different rotation speeds from 225 to 2500 rpm in the potential range between -1.0 and 0 V (Fig. S7). From the LSV curves at different rotation speeds, the electron transfer number (n) and kinetic-limiting current density (J_k) can be determined on the basis of Koutecky–Levich (K–L) equation as follows:^{S5}

$$\frac{1}{J} = \frac{1}{J_k} + \frac{1}{J_d} = \frac{1}{J_k} + \frac{1}{B\omega^{1/2}} \quad (\text{S1})$$

$$B = 0.62nFD_O^{2/3}\nu^{-1/6}C_O \quad (\text{S2})$$

where J is the measured limiting current density, J_k is the limiting kinetic current density, J_d is the limiting diffusion current density, ω is the angular velocity of the disk ($\omega = 2\pi N$, N is the linear rotation speed in rpm), F is the Faraday constant (96485 C mol^{-1}), D_O is the diffusion coefficient of O_2 ($1.90 \times 10^{-5} \text{ cm}^2 \text{ s}^{-1}$), ν is the kinematic viscosity of the electrolyte ($0.01 \text{ cm}^2 \text{ s}^{-1}$), and C_O is the bulk concentration of O_2 ($1.20 \times 10^{-6} \text{ mol cm}^{-3}$). The constant 0.62 is adopted when the rotation speed is expressed in radian per second (rad s^{-1}). According to Eqn. (S1) and (S2), the n and J_k values can be calculated from the slope and intercept at the y -axis of the K–L plots, respectively.

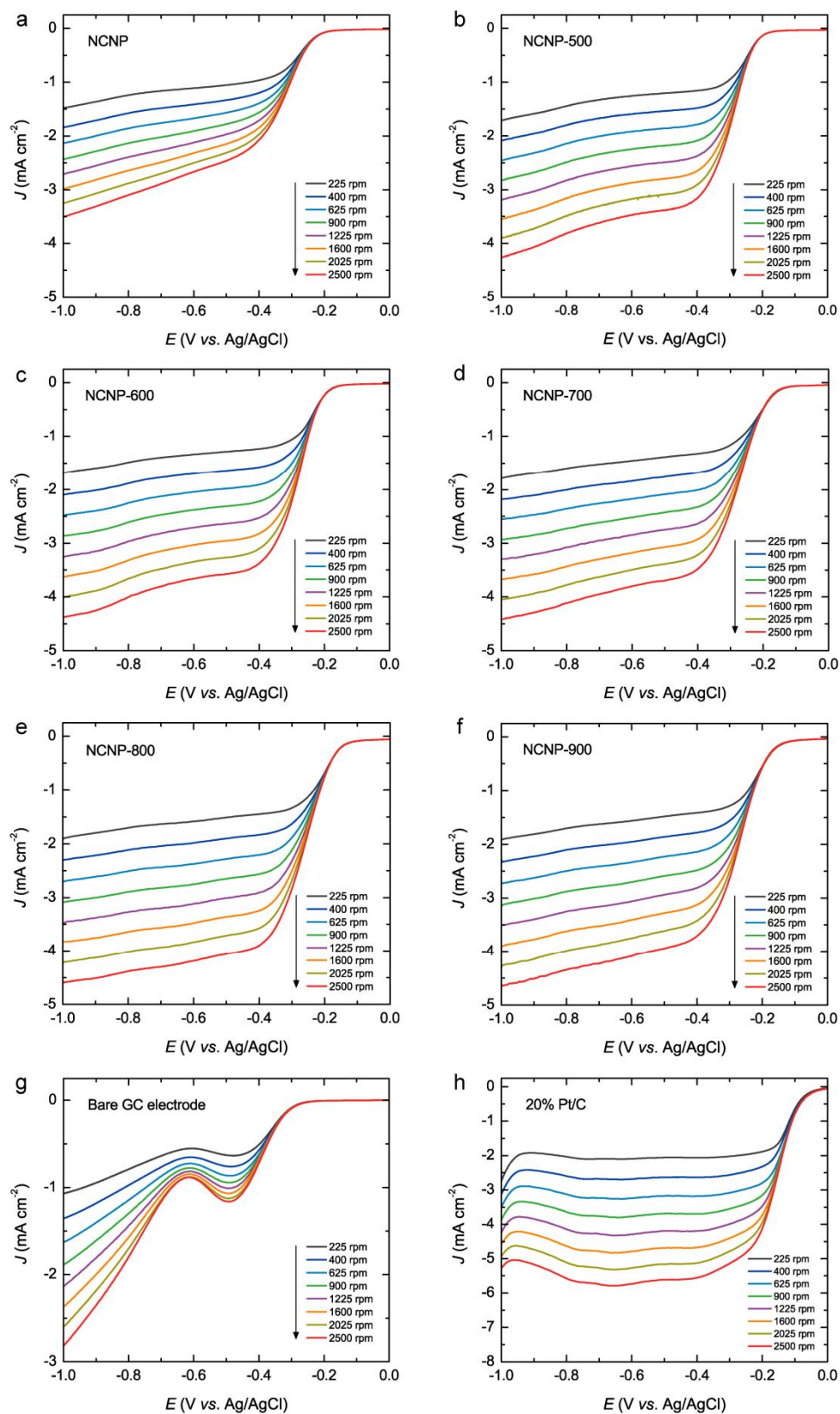


Fig. S7 LSV curves of the ORR for various catalysts in an O_2 -saturated 0.1 M KOH solution at different rotation speeds from 225 to 2500 rpm (10 mV s^{-1}): (a) NCNP, (b) NCNP-500, (c) NCNP-600, (d) NCNP-700, (e) NCNP-800, (f) NCNP-900, (g) bare GC electrode, and (h) 20% Pt/C.

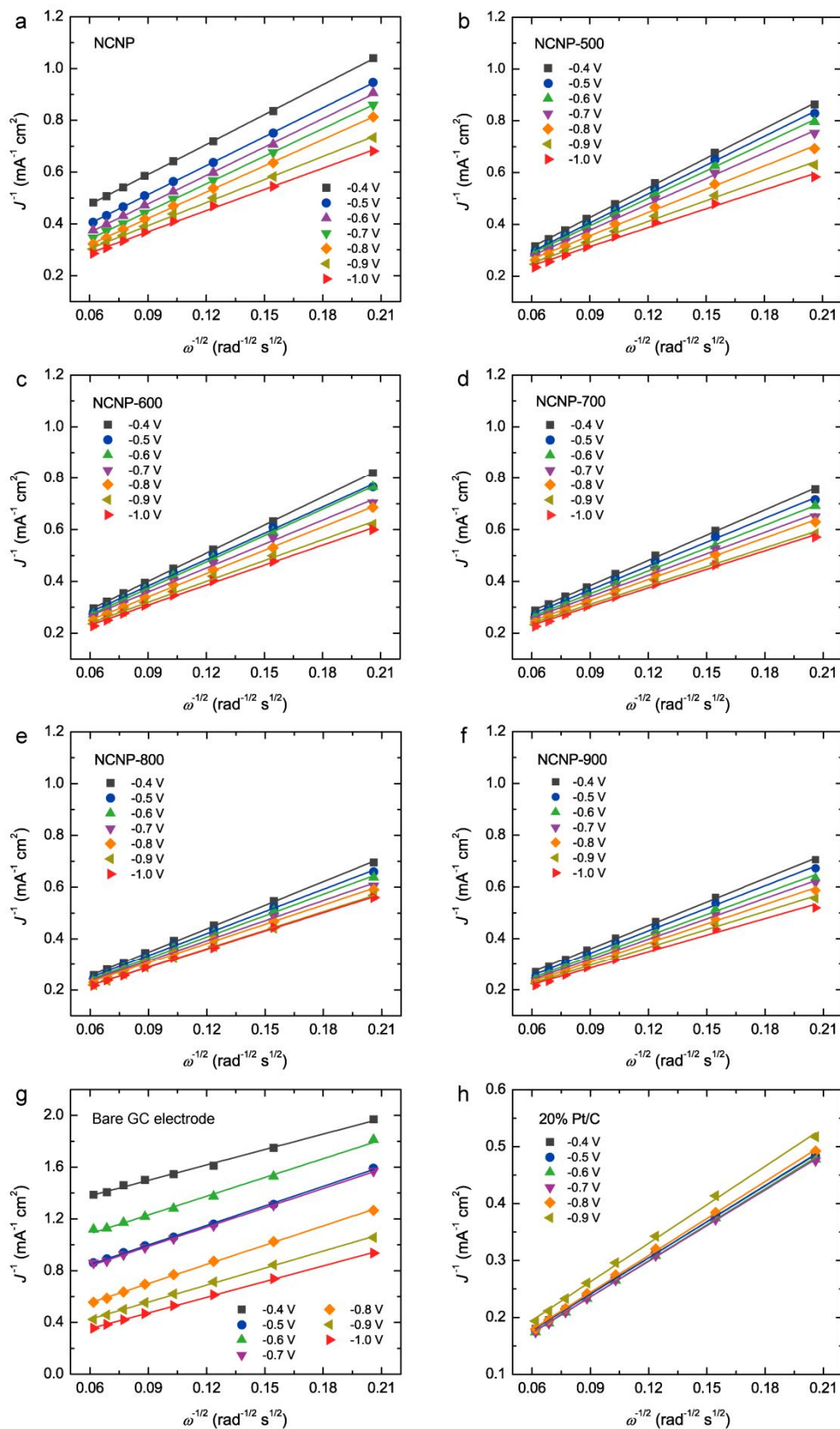


Fig. S8 The K–L plots of various catalysts obtained from the LSV data in Fig. S7 at the potentials from -1.0 to -0.4 V: (a) NCNP, (b) NCNP-500, (c) NCNP-600, (d) NCNP-700, (e) NCNP-800, (f) NCNP-900, (g) bare GC electrode, and (h) 20% Pt/C.

Rotating-ring disk electrode (RRDE) measurement

A certain amount of 10 μL of catalyst ink was applied onto a rotating ring-disk electrode (RRDE), which consists of a glassy carbon disk (disk diameter: 4 mm, $A = 0.126 \text{ cm}^2$) surrounded by a Pt ring (inner/outer-ring diameter: 5.0/7.0 mm). The catalyst loading is approximately $0.4 \text{ mg}_{\text{cat}} \text{ cm}^{-2}$.

To investigate the ORR mechanisms and kinetics occurred over the catalysts, the LSV measurements were performed on a catalyst-modified GC-RRDE at a rotation speed of 1600 rpm with a scan rate of 10 mV s^{-1} . The corresponding ring current was simultaneously measured with a Pt ring electrode by applying a constant potential of 0.5 V. The electron transfer number (n) per O_2 molecule involved in the ORR and the percentage of O_2 molecules that are reduced to HO_2^- can be calculated based on the ring and disk currents (Fig. S9) using the following equations:^{S6,S7}

$$n = 4 \times \frac{I_d}{I_d + I_r / N} \quad (\text{S3})$$

$$\text{HO}_2^- \% = 200 \times \frac{I_r / N}{I_d + I_r / N} \quad (\text{S4})$$

where I_d and I_r are the disk and ring currents, respectively. N is the collection efficiency. The N value in our system was calibrated in 0.1 M KOH with a 10 mM $\text{K}_3\text{Fe}(\text{CN})_6$ electrolyte, which was estimated to be approximately 0.43.

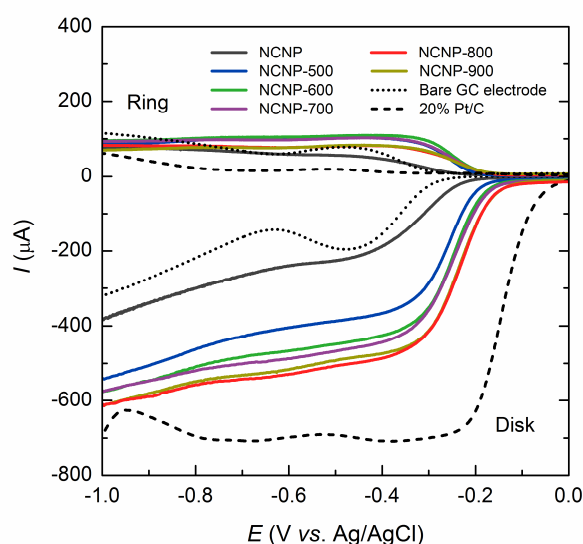


Fig. S9 Disk and ring currents on a RRDE for various catalysts in an O_2 -saturated 0.1 M KOH at a rotation speed of 1600 rpm (10 mV s^{-1}).

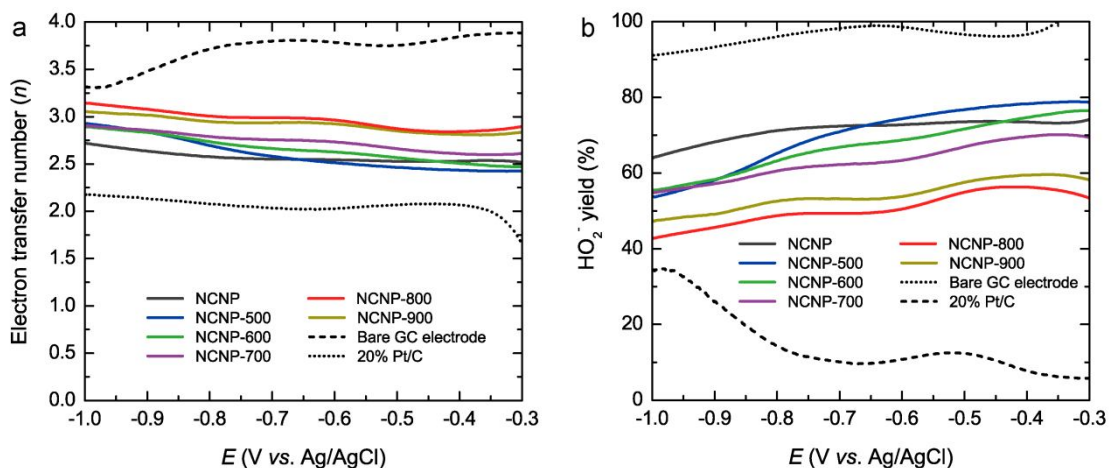


Fig. S10 (a) The calculated electron transfer number (n) and (b) HO_2^- yields for various catalysts as a function of potential.

Durability test

To confirm the durability of the catalyst, current-time ($I-t$) chronoamperometric responses were performed on a catalyst-modified GC-RDE at a rotation speed of 1600 rpm in an O_2 -saturated 0.1 M KOH solution by applied a constant potential of -0.4 V for 40000 s. The resistance to methanol crossover effect was examined by the introduction of 3.0 M methanol during the measurement of $I-t$ chronoamperometric responses.

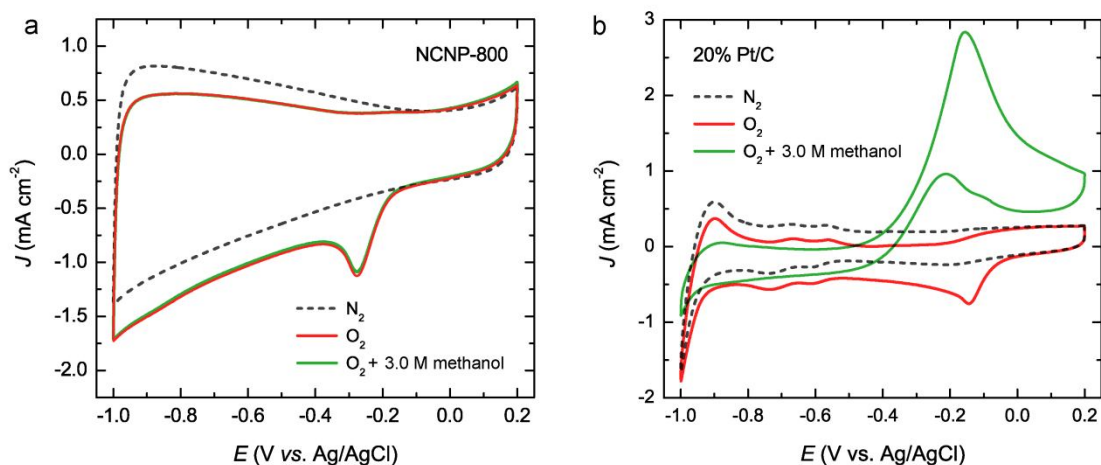


Fig. S11 Comparative CV curves with and without the introduction of 3.0 M methanol of (a) NCNP-800 and (b) 20% Pt/C.

References

- S1 G. Beamson and D. Grigg, High resolution XPS of organic polymers. The scienta ESCA A300 database, Chichester: Wiley 1992.
- S2 A. Valázquez-Palenzuela, L. Zhang, L. Wnag, P. L. Cabot, E. Brillas, K. Tsay and J. Zhang, *J. Phys. Chem. C*, 2011, **115**, 12929.
- S3 V. Datsynk, M. Kalyva, K. Papagelis, J. Parthenios, D. Tasis, A. Siokou, I. Kallitsis and C. Galiotis, *Carbon*, 2008, **46**, 833.
- S4 C.-M. Chen, J.-Q. Huang, Q. Zhang, W.-Z. Gong, Q.-H. Yang, M.-Z. Wang and Y.-G. Yang, *Carbon*, 2012, **50**, 659.
- S5 S. Treimer, A. Tang and D. C. Johnson, *Electroanal.*, 2002, **14**, 165.
- S6 A. Bonakdarpour, M. Lefevre, R. Yang, F. Jaouen, T. Dahn, J.-P. Dodelet and J. R. Dahn, *Electrochem. Solid State Lett.*, 2008, **11**, B105.
- S7 X. Li, H.-J. Zhang, H. Li, C. Deng and J. Yang, *ECS Electrochem. Lett.*, 2014, **3**, H33.